AGU PUBLICATIONS

Geochemistry, Geophysics, Geosystems

RESEARCH ARTICLE
10.1002/2014GC005376

Key Points:
- Cosmogenic exposure ages show the problem of the $^{40}Ar/^{39}Ar$ age of Lonar crater
- Patterns of surface exposure ages provide information of erosion status
- Coupling more than two dating methods can provide precise crater ages

Correspondence to:
Y. Yokoyama,
yokoyama@aori.u-tokyo.ac.jp

Citation:
Nakamura, A., Y. Yokoyama, Y. Sekine, K. Goto, G. Komatsu, P. S. Kumar, H. Matsuzaki, I. Kaneoka, and T. Matsui (2014), Formation and geomorphologic history of the Lonar impact crater deduced from in situ cosmogenic ^{10}Be and ^{26}Al, *Geochem. Geophys. Geosyst.*, *15*, 3190–3197, doi:10.1002/2014GC005376.

Received 9 APR 2014
Accepted 13 JUL 2014
Accepted article online 16 JUL 2014
Published online 19 AUG 2014

Formation and geomorphologic history of the Lonar impact crater deduced from in situ cosmogenic ^{10}Be and ^{26}Al

Atsunori Nakamura[1,2], Yusuke Yokoyama[1,2,3], Yasuhito Sekine[4], Kazuhisa Goto[5], Goro Komatsu[6], P. Senthil Kumar[7], Hiroyuki Matsuzaki[8], Ichiro Kaneoka[9], and Takafumi Matsui[10]

[1]Atmosphere and Ocean Research Institute, University of Tokyo, Kashiwa, Japan, [2]Department of Earth and Planetary Science, Graduate School of Science, University of Tokyo, Bunkyo-ku, Japan, [3]Institute of Biogeoscience, Japan Agency of Marine Science and Technology, Yokosuka, Japan, [4]Department of Complexity Science and Engineering, University of Tokyo, Kashiwa, Japan, [5]International Research Institute of Disaster Science, Tohoku University, Aoba-ku, Japan, [6]International Research School of Planetary Sciences, Università d'Annunzio, Pescara, Italy, [7]National Geophysical Research Institute, Council of Scientific and Industrial Research, Hyderabad, India, [8]Department of Nuclear Engineering and Management, University of Tokyo, Bunkyo-ku, Japan, [9]Earthquake Research Institute, University of Tokyo, Bunkyo-ku, Japan, [10]Planetary Exploration Research Center, Chiba Institute of Technology, Narashino, Japan

Abstract The Lonar impact crater is one of a few craters on Earth formed directly in basalt, providing a unique opportunity to study an analog for crater degradation processes on Mars. Here we present surface ^{10}Be and ^{26}Al exposure dates in order to determine the age and geomorphic evolution of Lonar crater. Together with a ^{14}C age of preimpact soil, we obtain a crater age of 37.5 ± 5.0 ka, which contrasts with a recently reported and apparently older $^{40}Ar/^{39}Ar$ age (570 ± 47 ka). This suggests that the $^{40}Ar/^{39}Ar$ age may have been affected by inherited radiogenic ^{40}Ar ($^{40}Ar^*_{inherited}$) in the impact glass. The spatial distribution of surface exposure ages of Lonar crater differs from that for Barringer crater, indicating Lonar crater rim is actively eroding. Our new chronology provides a unique opportunity to compare the geomorphological history of the two craters, which have similar ages and diameters, but are located in different climate and geologic settings.

1. Introduction

Lonar crater is a 1.88 km diameter crater located on the Deccan basaltic traps in India (Figures 1a–1c), which provides a rare opportunity to study an impact structure similar to those observed on the basaltic surfaces of Mars and other planets [*Fredriksson et al*., 1973]. Given that the age of terrestrial impact structures is key to understanding geomorphological processes following the impact, various dating methods have been applied to Lonar crater. However, a large discrepancy between different dating methods (1.79–570 ka) has been obtained. The ages can be classified into two groups. Relatively young ages (1.79–52 ka) have been obtained from radiocarbon dating of preimpact soil (1.79 ± 0.04–40.8 ± 1.1 ka) [*Maloof et al*., 2010], fission-track dating of impact glass (15.3 ± 13.3 ka) [*Storzer and Koeberl*, 2004], and thermoluminescence dating of impact glass (52 ± 6 ka) [*Sengupta et al*., 1997]. However, an old age (570 ka) was obtained from $^{40}Ar/^{39}Ar$ dating of melt rock [*Jourdan et al*., 2011]. The latter study concluded that the previously reported young ages are biased by secondary processes, such as contamination (radiocarbon) and alteration due to chemical weathering and/or wildfire (fission-track and thermoluminescence). However, $^{40}Ar/^{39}Ar$ dating of impact melt can also be potentially comprised by inherited radiogenic ^{40}Ar ($^{40}Ar^*_{inherited}$), which would make the measured $^{40}Ar/^{39}Ar$ ages erroneously old [*Jourdan et al*., 2007]. As such, the age of Lonar crater remains debated and requires verification using alternative approaches.

Terrestrial in situ cosmogenic nuclides (TCN) are produced within the upper few metres of Earth's surface by reacting with secondary cosmic rays. Since production rates of TCN are a function of altitude and latitude, it is possible to convert measured concentration into exposure ages [*Lal*, 1991]. Such ages represent minimum exposure ages, given the assumption of no erosion. A maximum erosion rate can also be calculated from the concentration of TCN, which can be used to reconstruct the original morphology of the crater. Although TCN have successfully been used to date Barringer crater in Arizona [*Nishiizumi et al*., 1991; *Phillips et al*., 1991], no other dates of impact craters based on TCN have been published. Here we compare

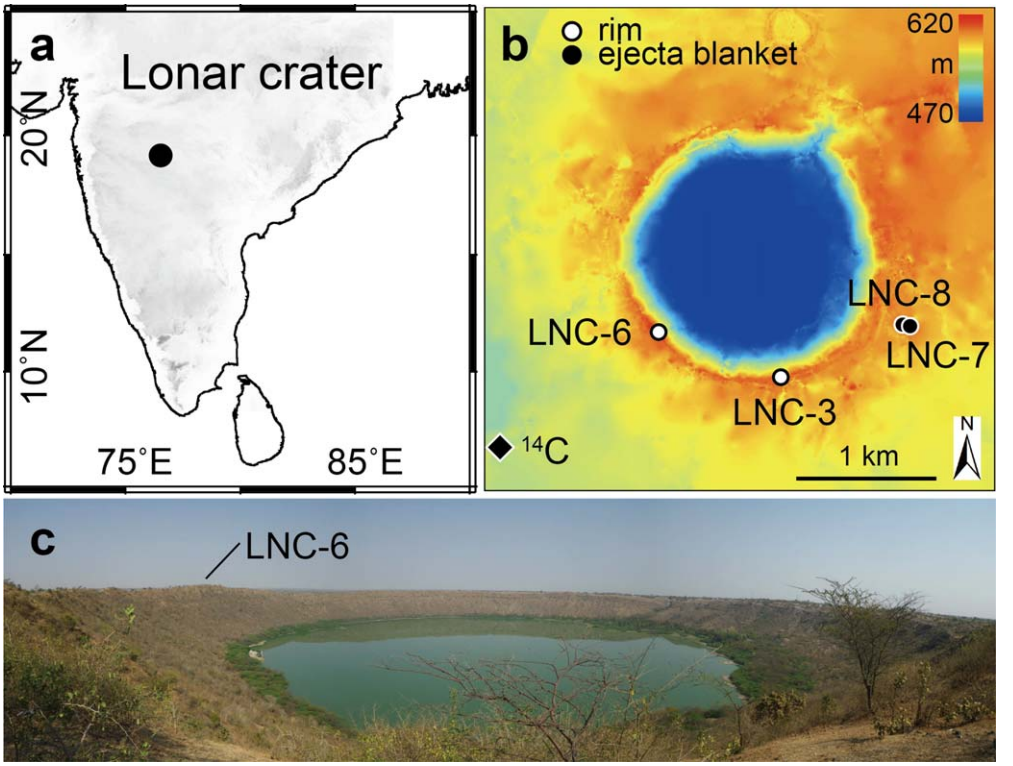

Figure 1. Location of Lonar crater and sampling point around the crater. (a) Location map. (b) Topography of Lonar crater and sampling locations. The topography was taken from digital elevation models [*Maloof et al.*, 2010]. (c) View of Lonar crater.

spatial age distributions observed from Lonar crater with those of Barringer crater, and describe the differing geomorphological histories experienced by these two craters under different climatic and geological settings.

2. Sampling Strategy

Lonar crater has a relatively pristine geomorphology, but does show some evidence of erosion [*Fudali et al.*, 1980; *Komatsu et al.*, 2014]. The current average height of the rim is 30 m, which is lower than the original height [*Maloof et al.*, 2010]. The slope of the inner crater wall (135 m deep) is 26° [*Fudali et al.*, 1980], and gullies and debris flows indicate degradation has occurred [*Komatsu et al.*, 2014]. An ejecta blanket extends on average 1350 m outward from the crater rim, with channel incisions located radially away from the crater rim [*Komatsu et al.*, 2014].

The objective of our study was to determine the ages of the oldest surfaces, given that TCN ages represent a minimum age of the cratering event. At Barringer crater, samples from the rim and ejecta blanket show approximately the same exposure ages as the cratering event [*Nishiizumi et al.*, 1991; *Phillips et al.*, 1991]. Thus, four quartz pebbles (4–7 cm in major axis) were sampled from summits of the rim and topographic high on the ejecta blanket of Lonar crater (Figures 1b, 2a–2e, and Table1). It should be noted that higher nuclide activities (older exposure ages and/or slow erosion rates) are often reported from such local topographic highs [*Bierman and Caffee*, 2002; *Hancock and Kirwan*, 2007; *Nakamura et al.*, 2014]; therefore, relatively older surfaces are expected to be found from tops of the landform. Quartz pebbles are angular and have a layered form, indicating an origin from quartz vugs or veins in the target basalt. Based on observations of the crater wall, accumulation of TCN prior to the cratering event should have been minimal, because these samples were almost completely shielded from cosmic rays by the basalt prior to the impact. Quartz vugs or veins are observed at much greater depths than potential cosmic ray penetration at the vesicular margins of five basalt flows that make up the target rock [*Maloof et al.*, 2010]. Quartz pebbles

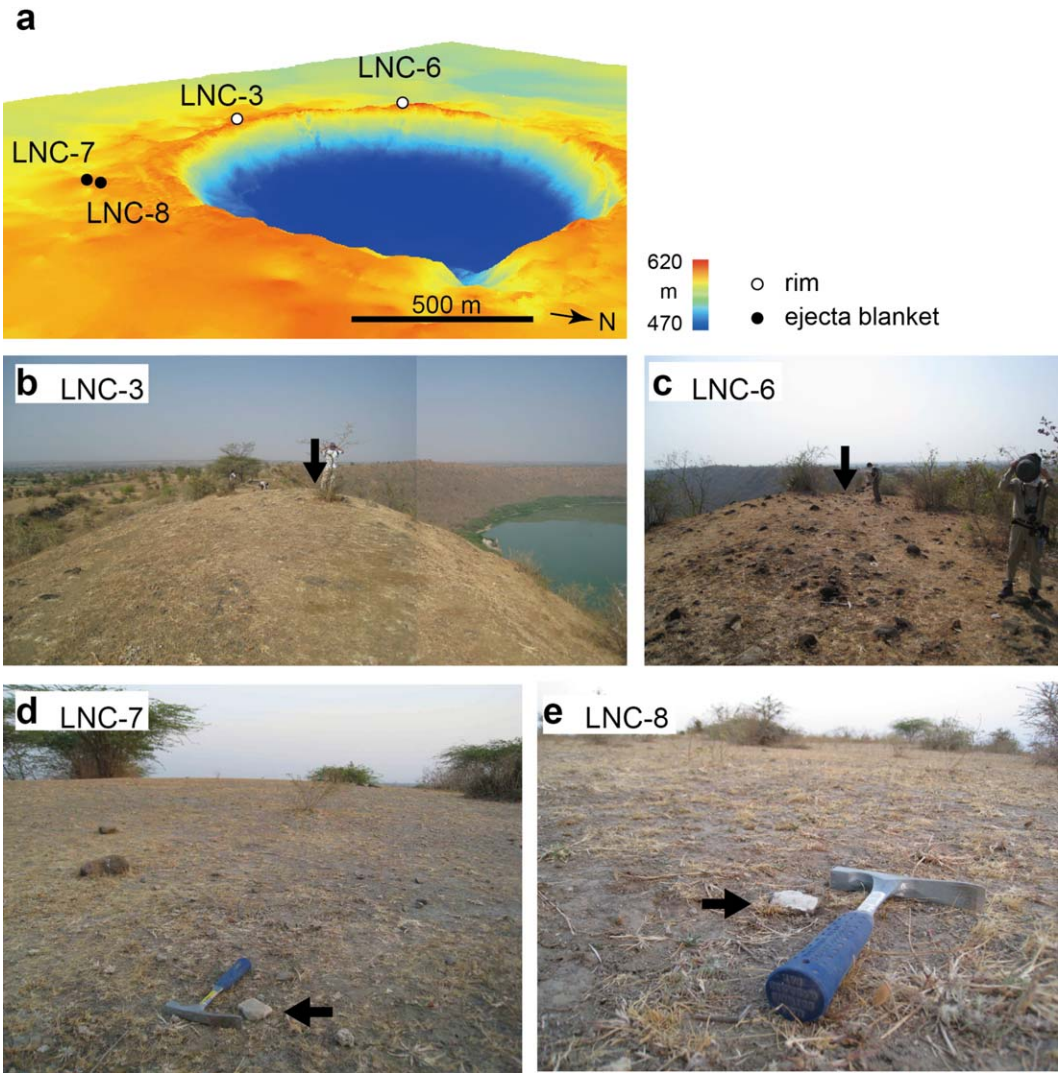

Figure 2. Images showing sampling locations. (a) Topography of Lonar crater and sampling locations. The topography was taken from digital elevation models. (b) Photograph of sampling site LNC-3 on the crater rim. Arrow shows the sampling point. (c) Photograph of sampling site LNC-6 on the crater rim. (d) Photograph of sampling site LNC-7 on the ejecta blanket. Arrow shows the analyzed quartz pebble. (e) Photograph of sampling site LNC-8.

LNC-3 and -6 are from the summits of the southern and southwestern rims of the crater (Figures 1b and 2a–2c), respectively. LNC-7 and -8 were sampled from an eastern ejecta blanket hill (Figures 1b, 2d, and 2e), which is isolated by surrounding channel erosion.

To compare with minimum exposure ages from TCN, ^{14}C ages were determined on preimpact soil resampled from the Kalapani Dam site (Figures 1b and 3), which is the same outcrop as that dated previously by *Maloof et al*. [2010]. At this site, preimpact black soil with patches of white carbonate is overlain by impact ejecta (1.5 m thick). As authigenic carbonate in soil can be precipitated a long time after soil formation, we performed ^{14}C dating of bulk organic matter and carbonate separately [*Yokoyama et al*., 2007]. The ^{14}C age of bulk

Table 1. Location and Description of Cosmogenic Nuclide Samples

Sample	Latitude (°N)	Longitude (°E)	Altitude (m)	Sample Size (cm)
LNC-3	19.9686	76.5104	620	7 × 3 × 2
LNC-6	19.9716	76.5020	630	7 × 5 × 2
LNC-7	19.9718	76.5194	600	5 × 5 × 2
LNC-8	19.9718	76.5189	600	4 × 3 × 2

Figure 3. Lithological column and photograph of the outcrop where the ^{14}C samples were obtained. Pre-impact black soil with patches of white carbonate are overlain by impact ejecta (1.5 m thick).

organic matter provides a maximum limit on the age of impact, given that organic matter can inherit old carbon [*Trumbore*, 2000; *Nakamura et al*., 2012]. We present the ages of the crater using both minimum and maximum respectively using TCN and stratigraphically constrained radiocarbon.

3. Methods

Quartz pebbles were crushed to 0.35–1.00 mm in size, and subsequently separated by chemical etching following the method of *Kohl and Nishiizumi* [1992]. The purified quartz grains (20–40 g) were dissolved in HF acid and spiked with a Be carrier (~0.2 mg). Aliquots for Be and Al analysis were separated by column chromatography and stable ^{27}Al was measured by inductively coupled plasma-atomic emission spectrometry (ICP-AES). Samples were then oxidized for accelerator mass spectrometry (AMS) measurements at the University of Tokyo, Japan. The standards used were KNB5-1 for ^{10}Be ($^{10}Be/^{9}Be = 2.709 \times 10^{-11}$) [*Nishiizumi et al*., 2007] and KNA4-2 for ^{26}Al ($^{26}Al/^{27}Al = 3.096 \times 10^{-11}$) [*Nishiizumi*, 2004]. ^{10}Be and ^{26}Al backgrounds were subtracted using the values of procedural blanks ($1.781 \pm 0.179 \times 10^{-14}$ and $8.515 \pm 0.852 \times 10^{-16}$ for ^{10}Be and ^{26}Al, respectively). The 1σ errors on the determined concentrations include counting errors on the sample, standard, and procedural blank (Table 1). Exposure ages were calculated using the CRONUS online calculator version 2.2 [*Balco et al*., 2008]. We used a density of 2.7 g/cm^3 and sample thickness of 2 cm. A shielding correction was not used and does not significantly affect the calculated ages. The time-dependent models of *Lal* [1991] and *Stone* [2000] were used for the production model [*Balco et al*., 2008]. A value of 62 year was subtracted from the exposure ages to correct ages to ka (present = A.D. 1950).

Bulk organic matter and carbonate in the soil were analyzed separately. The sample of bulk organic matter was pretreated in 1 M HCl to remove carbonate. The ^{14}C dates were calibrated to calendar years (Table 2) using the calibration software Oxcal v3.10 [*Bronk Ramsey*, 2001] with the Intcal09 dataset [*Reimer et al*., 2009].

4. Results and Discussion

4.1. The Age of Lonar Crater

Ages derived from both ^{10}Be and ^{26}Al are consistent within 1σ, suggesting the measurements are robust (Table 2). $^{26}Al/^{10}Be$ ratios are typical of a single exposure history (Figure 4). The oldest sample is LNC-7 from the ejecta blanket (37.5 ± 5.0 ka for ^{10}Be; 37.4 ± 3.4 ka for ^{26}Al), whereas another sample from the ejecta

Table 2. Cosmogenic Nuclide Data and Exposure Ages of Lonar Crater[a]

Sample	Dissolved quartz (mg)	Be Carrier (mg)	^{27}Al (ppm)	$^{10}Be/^{9}Be$ (10^{-14})	1σ Error	^{10}Be (10^4 atoms/g)	1σ Error	$^{26}Al/^{27}Al$ (10^{-14})	1σ Error	^{26}Al (10^5 atoms/g)	1σ Error	^{10}Be Exposure Age (ka)	1σ Error	^{26}Al Exposure Age (ka)	1σ Error
LNC-3	19593.95	1955.07	187	4.787	0.485	3.192	0.323	4.014	0.627	1.678	0.262	6.1	0.8	4.9	0.9
LNC-6	43322.80	1978.66	219	16.166	1.639	4.934	0.500	6.336	0.320	3.094	0.156	9.3	1.2	8.6	0.9
LNC-7	21251.82	1969.93	330	34.868	3.534	21.598	2.189	19.885	0.608	14.662	0.448	37.5	5.0	37.7	3.4
LNC-8	32609.89	1967.58	199	7.596	0.770	3.063	0.310	4.420	0.338	1.965	0.150	6.0	0.8	5.7	0.7

[a]The time-dependent model of *Lal* [1991] and *Stone* [2000] was used for the production model [*Balco et al*., 2008]. A value of 62 year was subtracted from the exposure ages to correct ages to ka (present = A.D. 1950).

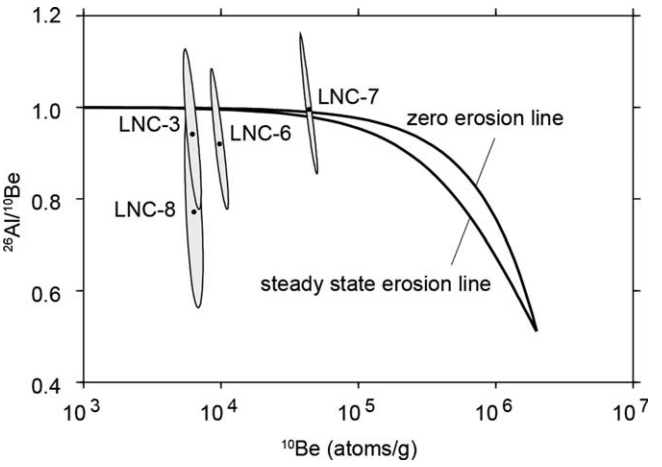

Figure 4. Plot of ^{26}Al/^{10}Be versus ^{10}Be concentration. The plot was constructed using the CRONUS online calculator version 2.2 [*Balco et al.*, 2008]. ^{10}Be concentrations were normalized to values at sea level and high latitude. ^{26}Al/^{10}Be was normalized to production rates. Zero and steady state erosion lines are shown as solid lines.

blanket (LNC-8) yielded much younger ages (6.0 ± 0.8 ka for ^{10}Be; 5.7 ± 0.7 ka for ^{26}Al). In contrast, samples from the rim (LNC-3 and −6) both yield Holocene ages ranging from 4.9 ± 0.9 to 9.3 ± 1.2 ka (Figures 5a and 5b). Therefore, our best estimate of the minimum age of Lonar crater is ~37.5 ka. As a result, three of the four samples with anomalously young ages indicate erosional removal of material at their sampling sites (Figures 5a and 5b).

Although the sampling sites of LNC-7 and −8 are within 100 m of each other on the ejecta blanket, these samples have large age differences, possibly due to quartz enrichment on the surface of the ejecta blanket resulting from selective erosion of material. Such variations of TCN concentrations in surface quartz pebbles have been reported from eroded fluvial terraces that comprise unsorted grains [*Hein et al.*, 2009, *Molliex et al.*, 2013]. Quartz pebbles are resistant to erosional and weathering processes as compared with other components of the ejecta, such as fragments of host basalt and impact glass. Hence, once a buried quartz pebble is exposed at the surface, the quartz tends to remain there, thereby increasing the TCN concentration. Our results indicate differences in the duration of exposure of the two measured quartz pebbles to

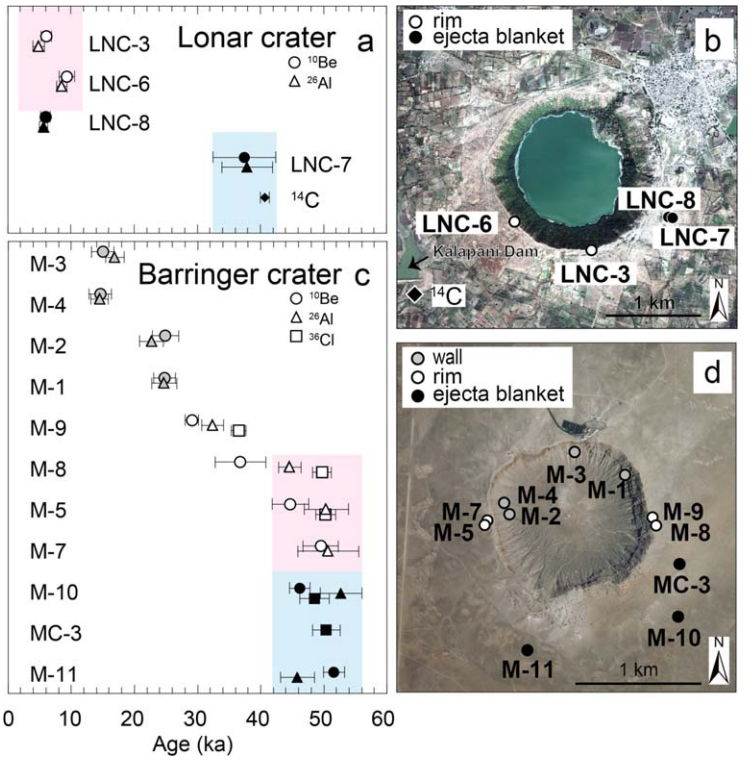

Figure 5. Spatial age distributions and satellite images. (a) Exposure ages and ^{14}C age from Lonar crater. LNC-7 provides a minimum age for the crater. The ^{14}C age provides a maximum age for the crater. (b) Quickbird image of Lonar crater [*Maloof et al.*, 2010] and sampling localities. (c) Compiled exposure ages for the Barringer crater [^{10}Be and ^{26}Al; *Nishiizumi et al.*, 1991, ^{36}Cl; *Phillips et al.*, 1991]. (d) Landsat image of Barringer crater (http://www.lpi.usra.edu/publications/books/barringer_crater_guidebook/landsat/).

Table 3. Radiocarbon Ages and Calendar Ages of the Soil Samples[a]

Dated Material	$\delta^{13}C$ (‰)	Radiocarbon Age (BP)	Error	Calendar Age (cal yr BP)	Error (2σ)
Bulk organic matter	−16.1	35480	260	40700	680
Soil carbonate	−15.7	3880	50	4285	135

[a]Bulk organic matter and carbonate in the soil were analyzed separately.

cosmic rays. As such, the quartz pebbles are ideal material from which to obtain the age of the ejecta, even if the surface is currently undergoing erosion. The presence of channels on the ejecta blanket extending radially away from the crater centre also indicates that active erosion has occurred after formation of the crater [*Komatsu et al*., 2014]. In contrast, two samples from different summits of the rim both yield Holocene ages. These ages may reflect continuous erosion of the crater rim. Maximum erosion rates calculated from the rim samples range from 96 to 203 mm/kyr, indicating the original rim height would have been 41–64 m (see section 4.3. for further discussion). Alternatively, the ages may indicate episodic collapse of the crater wall and rim during the Holocene, given that precipitation related to the Indian summer monsoon has intensified during the Holocene [*Sinha et al*., 2005].

The maximum crater age can be estimated from the ^{14}C age of bulk organic matter (40.7 ± 0.7 ka), and this age is consistent with the minimum exposure age (37.5 ± 5.0 ka for ^{10}Be; 37.4 ± 3.4 ka for ^{26}Al; LNC-7) (Figure 5b). Given that ^{14}C ages of bulk organic matter can be affected by relict material [*Trumbore* 2000; *Nakamura et al*., 2012], this age might overestimate the timing of the impact. However, the soil carbonate age of 4.29 ± 0.14 ka indicates that carbonate precipitation has occurred since preimpact soil formation (Table 3). This suggests that the ^{14}C ages from this outcrop reported previously by *Maloof et al*. [2010] (1.79 ± 0.04, 23.5 ± 0.20, and 27.5 ± 0.18 ka) might have been affected by secondary carbon contamination. If acid treatment does not completely remove soil carbonate, the resulting age can be erroneously young. Indeed, the ^{14}C ages of *Maloof et al*. [2010] are positively correlated with $\delta^{13}C$, suggesting recent carbon contamination. We cannot readily explain the youngest age (1.79 ± 0.04 ka) by carbonate contamination, but it could be due to heterogeneity of the soil carbonate or modern root contamination [*Maloof et al*., 2010]. In summary, the maximum age of the cratering event is 40.7 ± 0.7 ka. It is notable that a ^{14}C age from another site [*Maloof et al*., 2010], originally suspected to be erroneously old due to carbon contamination (40.8 ± 1.1 ka), is consistent with our result. The oldest minimum exposure age (TCN) and maximum cratering age (^{14}C) are in close agreement, indicating that LNC-7 was exposed at the surface almost immediately after impact. Therefore, we conclude that our ^{10}Be exposure age of 37.5 ± 5.0 ka is the best estimate of the age of Lonar crater. We use the ^{10}Be age of LNC-7 because it overlaps the ^{26}Al and ^{14}C ages within 1σ error (Figure 5b).

4.2. Reinterpretation of $^{40}Ar/^{39}Ar$ Data

Our exposure age, together with newly obtained ^{14}C ages of preimpact soil, suggests that a recently reported $^{40}Ar/^{39}Ar$ age (570 ± 47 ka) [*Jourdan et al*., 2011] was compromised by the presence of $^{40}Ar^*_{inherited}$ in the impact glass. An inverse Ar isochron can in fact be an apparent isochron caused by the random distribution of both $^{40}Ar^*_{inherited}$ and radiogenic $^{40}Ar^*$ in glassy materials and mixing with atmospheric Ar. *Jourdan et al*. [2011] argued that $^{40}Ar^*_{inherited}$ and radiogenic $^{40}Ar^*$ should be distinguishable, because radiogenic $^{40}Ar^*$ should be associated with K-rich sites, whereas $^{40}Ar^*_{inherited}$ should be homogeneously distributed. This interpretation is applicable for crystalline materials; however, it may not be the case for amorphous samples such as impact glass. In glassy materials, K has no preferential location site and would be randomly distributed like $^{40}Ar^*_{inherited}$. In such a case, $^{40}Ar^*_{inherited}$ and radiogenic $^{40}Ar^*$ would behave similarly during stepwise heating. Data reported by *Jourdan et al*. [2011] show relatively constant K/Ca values over a wide temperature range, indicating a similar random distribution of both K and Ca. This supports our inference concerning the distribution of $^{40}Ar^*_{inherited}$ and radiogenic $^{40}Ar^*$, because in crystalline basaltic material K and Ca would be expected to be generally located in different sites to each other. However, total atmospheric Ar includes components of both primary and secondary origin, which cannot be separated and are located at different sites to $^{40}Ar^*_{inherited}$ and radiogenic $^{40}Ar^*$. Hence, an apparent inverse isochron could be interpreted as a mixing line between $^{40}Ar^*_{inherited}$ and radiogenic $^{40}Ar^*$, and atmospheric Ar. Such apparent inverse isochron, exhibiting atmospheric values for axial intercepts, are reported in previous studies [*Pankhurst et al*., 1973; *Kaneoka and Aoki*, 1978; *Ozima et al*., 1989].

A thermoluminescence age of impact glass (52 ± 6 ka) [*Sengupta et al*., 1997] is also consistent with our results. Furthermore, the sedimentation rate obtained from a 10 m long core of sediments in the crater lake [*Anoop et al*., 2013] is consistent with our age when integrated to the full thickness of the lake sediment. In comparison, only $^{40}Ar/^{39}Ar$ results indicate an order of magnitude older age. The problem of $^{40}Ar^*_{inherited}$ in dating impact glass has also been reported for Tswaing impact crater, South Africa, where 0.015 to 4.15% incomplete degassing of the impact melt biased the $^{40}Ar/^{39}Ar$ age of the crater by a factor of 50 to 1000, yielding an erroneously old age [*Jourdan et al*., 2007]. Assuming the age of the target basalt was 65 Ma [*Kaneoka*, 1980], the percentage of incomplete degassing for Lonar crater can be calculated to be 0.8% using the equation described in *Jourdan et al*. [2007]. While the amount of $^{40}Ar^*_{inherited}$ strongly depends on target lithology, melt volume, and the temperature-time melt path, the value of 0.8% is comparable to the value estimated for the Tswaing impact crater [*Jourdan et al*., 2007]. Therefore, the reliability of $^{40}Ar/^{39}Ar$ ages of glassy impact material need to be carefully considered.

4.3. Original Height of the Crater Rim

Reconstruction of the initial crater geometry is important, and considerable debate exists as to the original height of the Lonar crater rim. Although we cannot fully exclude the possibility that the crater rim collapsed in the early Holocene, the minimum thickness of removed material at the sampling site is calculated to be 1–14 m, using the maximum erosion rates calculated for LNC-3 and LNC-6 (ranging from 96 to 203 mm/kyr). Adding the present height of the sampling site (40–50 m), the original height is calculated to be 41–64 m, which is in the same range as estimated by previous studies. Based on mass balance calculations of sediments in the crater floor recovered by drilling, *Fudali et al*. [1980] estimated the original rim height to be 40 m, which was linearly extrapolated from the current outer-rim crest slope to the original rim radius. Due to erosional degradation of the original rim crest slope, this extrapolation should be considered a lower limit. In contrast, *Maloof et al*. [2010] estimated the original rim height to be 60 m at the present-day rim radius of 940 m, using an empirical equation for the rim height of the crater.

4.4. Geomorphic Evolution of the Lonar Crater in Comparison to the Barringer Crater

The spatial distribution of ages at Lonar crater differs from that at Barringer crater [^{10}Be and ^{26}Al; *Nishiizumi et al*., 1991, ^{36}Cl; *Phillips et al*., 1991]. Our new chronology provides a unique opportunity to compare the geomorphological history of the two craters, which have similar ages and diameters, but are located in different settings (Figures 5a–5d). Samples from the rim and ejecta blanket of Barringer crater have approximately the same exposure ages as the cratering event, implying that the rim samples have not experienced significant erosion (Figure 5c). Young samples from the crater wall were exhumed or freshly eroded during the last glacial maximum [*Nishiizumi et al*., 1991]. In contrast, rim samples from Lonar crater are younger than the impact age, indicating that Lonar crater rim is actively eroding, and this highlights the different geomorphological history of the two craters under different climatic and geological settings. Modern annual precipitation around Lonar crater is 752 mm/yr [*Komatsu et al*., 2014], whereas precipitation at Barringer crater is 490 mm/yr (200 mm/yr of rainfall; 290 mm/yr of snowfall) [*Kumar et al*., 2010]. The target lithology might also affect modification of the craters, given that Lonar crater is on basalt, whereas the Barringer crater is on sandstone and limestone. Precipitation and lithology are the dominant controls on erosion rate [*von Blanckenburg et al*., 2005, *Ferrier et al*., 2013], and hence might affect the differences in the post impact modification of the two craters.

5. Conclusions

The Lonar impact crater is one of a few craters on Earth formed directly in basalt, providing a unique opportunity to study an analog for crater degradation processes on Mars. We present surface ^{10}Be and ^{26}Al exposure dates in order to determine the age and geomorphic evolution of Lonar crater. The minimum exposure ages of Lonar crater are 37.5 ± 5.0 ka for ^{10}Be and 37.4 ± 3.4 ka for ^{26}Al, respectively. These ages are consistent with maximum limit of the impact age obtained from ^{14}C ages of preimpact soil (40.7 ± 0.7 ka). Therefore, we conclude that our ^{10}Be exposure age of 37.5 ± 5.0 ka is the best estimate of the age of Lonar crater. We use the ^{10}Be age of LNC-7 because it overlaps the ^{26}Al and ^{14}C ages within 1σ error. Our results contrasts with a recently reported and apparently older $^{40}Ar/^{39}Ar$ age (570 ± 47 ka) [*Jourdan et al*., 2011], suggesting that the $^{40}Ar/^{39}Ar$ age may have been affected by inherited radiogenic ^{40}Ar ($^{40}Ar^*_{inherited}$) in the impact glass. The spatial distribution of surface exposure ages for Lonar crater differs from that for

Barringer crater indicating Lonar crater rim is actively eroding. Our new chronology provides a unique opportunity to compare the geomorphological history of the two craters, which have similar ages and diameters, but are located in different climate and geologic settings.

Acknowledgments
This work was supported by the JSPS NEXT program GR031 and GCOE program. We thank Y. Chang, Y. Miyairi, and A. Suzuki for their assistance, and S. P. Obrochta for discussions about the manuscript.

References

Anoop, A., S. Prasad, B. Plessen, N. Basavaiah, B. Gaye, R. Naaumann, P. Menzel, S. Weise, and A. Brauer (2013), Palaeoenvironmental implications of evaporative gaylussite crystals from Lonar Lake, central India, *J. Quat. Sci.*, *28*(4), 349–359, doi:10.1002/jqs.2625.

Balco, G., J. O. Stone, N. A. Lifton, and T. J. Dunai (2008), A complete and easily accessible means of calculating surface exposure ages or erosion rates from ^{10}Be and ^{26}Al measurements, *Quat. Geochronol.*, *3*(3), 174–195.

Bierman, P. R., and M. Caffee (2002), Cosmogenic exposure and erosion history of Australian bedrock landforms, *GSA Bull.*, *114*(7), 787–803.

Bronk Ramsey C. (2001), Development of the radiocarbon program OxCal, *Radiocarbon*, *43*, 355–363.

Ferrier, K. L., K. L. Huppert, and J. T. Perron (2013), Climatic control of bedrock river incision, *Nature*, *496*(7444), 206–209.

Fredriksson, K., A. Dube, D. J. Milton, and M. S. Balasund (1973), Lonar Lake, India: An impact crater in basalt, *Science*, *180*(4088), 862–864.

Fudali, R. F., D. J. Milton, K. Fredriksson, and A. Dube (1980), Morphology of Lonar Crater, India: Comparisons and implications, *Moon Planets*, *23*(4), 493–515.

Hancock, G., and M. Kirwan (2007) Summit erosion rates deduced from ^{10}Be: Implications for relief production in the Central Appalachians, *Geology*, *35*(1), 89–92.

Hein, A. S., N. R. J. Hulton, T. J. Dunai, C. Schnabel, M. R. Kaplan, M. Naylor, and S. Xu (2009), Middle Pleistocene glaciation in Patagonia dated by cosmogenic-nuclide measurements on outwash gravels, *Earth Planet. Sci. Lett.*, *286*(1-2), 184–197.

Jourdan, F., P. R. Renne, and W. U. Reimold (2007), The problem of inherited ^{40}Ar* in dating impact glass by the ^{40}Ar/^{39}Ar method: Evidence from the Tswaing impact crater (South Africa), *Geochim. Cosmochim. Acta*, *71*(5), 1214–1231.

Jourdan, F., F. Moynier, C. Koeberl, and S. Eroglu (2011), ^{40}Ar/^{39}Ar age of Lonar crater and consequence for the geochronology of planetary impacts, *Geology*, *39*(7), 671–674.

Kaneoka, I. (1980), ^{40}Ar–^{39}Ar dating on volcanic rocks of the Deccan Traps, India, *Earth Planet. Sci. Lett.*, *46*(2), 233–243.

Kaneoka, I., and K. Aoki (1978) ^{40}Ar/^{39}Ar analyses of phlogopite nodules and phlogopite-bearing peridotites in South African kimberlites, *Earth Planet. Sci. Lett.*, *40*(1), 119–129.

Komatsu, G., P. S. Kumar, K. Goto, Y. Sekine, C. Giri, and T. Matsui (2014), Drainage systems of Lonar Crater, India: Contributions to Lonar Lake hydrology and crater degradation, *Planet. Space Sci.*, *95*, 45–55.

Kohl, C. P., and K. Nishiizumi (1992), Chemical isolation of quartz for measurement of in-situ-produced cosmogenic nuclides, *Geochim. Cosmochim. Acta*, *56*(9), 3583–3587.

Kumar, P. S., J. W. Head, and D. A. Kring (2010), Erosional modification and gully formation at Meteor Crater, Arizona: Insights into crater degradation processes on Mars, *Icarus*, *208*(2), 608–620.

Lal, D. (1991), Cosmic ray labeling of erosion surfaces: in situ nuclide production rates and erosion models, *Earth Planet. Sci. Lett.*, *104*(2-4), 424–439.

Maloof, A. C., S. T. Stewart, B. P. Weiss, S. A. Soule, N. L. Swanson-Hysell, K. L. Louzada, I. Garrick-Bethell, and P. M. Poussart (2010), Geology of Lonar Crater, India, *Geol. Soc. Am. Bull.*, *122*(1-2), 109–126.

Molliex, S., L. L. Siame, D. L. Bourles, O. Bellier, R. Braucher, and G. Clauzon (2013), Quaternary evolution of a large alluvial fan in a periglacial setting (Crau Plain, SE France) constrained by terrestrial cosmogenic nuclide (^{10}Be), *Geomorphology*, *195*, 45–52.

Nakamura, A., et al. (2012), Late Holocene Asian monsoon variations recorded in Lake Rara sediment, western Nepal, *J. Quat. Sci.*, *27*(2), 125–128, doi:10.1002/jqs.1568.

Nakamura, A., Y. Yokoyama, K. Shiroya, Y. Miyairi, and H. Matsuzaki (2014), Direct comparison of site-specific and basin-scale erosion rate estimation by in-situ cosmogenic nuclides: An example from the Abukuma Mountains, Japan, *Prog. Earth Planet. Sci.*, *1*, 9, doi:10.1186/2197-4284-1-9.

Nishiizumi, K. (2004), Preparation of ^{26}Al AMS standards, *Nucl. Insttum. Methods Phys. Res. Sect. B*, *223*, 388–392.

Nishiizumi, K., C. P. Kohl, E. M. Shoemaker, J. R. Arnold, J. Klein, D. Fink, and R. Middleton (1991), In situ ^{10}Be–^{26}Al exposure ages at Meteor Crater, Arizona, *Geochim. Cosmochim. Acta*, *55*(9), 2699–2703.

Nishiizumi, K., M. Imamura, M. W. Caffee, J. R. Southon, R. C. Finkel, and J. McAninch (2007), Absolute calibration of ^{10}Be AMS standards. *Nucl. Instrum. Methods Phys. Res. Sect. B*, *258*, 403–413.

Ozima, M., S. Zashu, Y. Takigami, and G. Turner (1989), Origin of the anomalous 40Ar-39Ar age of Zaire cubic diamonds: Excess ^{40}Ar in pristine mantle fluids, *Nature*, *337*, 226–229.

Pankhurst, R. J., S. Moorbath, D. C. Rex, and G. Turner (1973), Mineral age patterns in ca. 3700 my old rocks from west Greenland, *Earth Planet. Sci. Lett.*, *20*(2) 157–170.

Phillips, F. M., M. G. Zreda, S. S. Smith, D. Elmore, P. W. Kubik, R. I. Dorn, and D. J. Roddy (1991), Age and geomorphic history of Meteor Crater, Arizona, from cosmogenic ^{36}Cl and ^{14}C in rock varnish, *Geochim. Cosmochim. Acta*, *55*(9), 2695–2698.

Reimer, P. J., et al. (2009), INTCAL09 and MARINE09 radiocarbon age calibration curves, 0–50,000 years cal BP, *Radiocarbon*, *51*(4), 1111–1150.

Sengupta, D., N. Bhandari, and S. Watanabe (1997), Formation age of Lonar Meteor Crater, India, *Revista de Fisica Aplicada e Instrumentacao*, *12*, 1–7.

Sinha, A., K. G. Cannariato, L. D. Stott, H. C. Li, C. F. You, H. Cheng, R. L. Edwards, and I. B. Singh (2005), Variability of southwest Indian summer monsoon precipitation during the Bolling-Allerod, *Geology*, *33*(10), 813–816.

Stone, J. O. (2000), Air pressure and cosmogenic isotope production, *Journal of Geophysical Research-Solid Earth*, *105*, 23753–23759.

Storzer, D. and C. Koeberl (2004), Age of Lonar impact Crater, India: First results from fission track dating, paper presented at 35th Lunar Planetary Science Conference, abstract 1309, Lunar and Planetary Institute, Houston.

Trumbore, S. (2000), Age of soil organic matter and soil respiration: Radiocarbon constraints on belowground C dynamics, *Ecol. Appl.*, *10*(2), 399–411.

von Blanckenburg, F. (2005), The control mechanisms of erosion and weathering at basin scale from cosmogenic nuclides in river sediment, *Earth Planet. Sci. Lett.*, *237*(3-4), 462–479.

Yokoyama, Y., Y. Miyairi, H. Matsuzaki, and F. Tsunomori (2007), Relation between acid dissolution time in the vacuum test tube and time required for graphitization for AMS target preparation, *Nucl. Instrum. Methods Phys. Res. Sect. B*, *259*(1), 330–334.